Influence of Microstructure on Mechanical Properties of Snow

K.C. Agrawal

Snow & Avalanche Study Establishment, Manali

and

R.K. Mittal

Indian Institute of Technology, New Delhi-110 060

ABSTRACT

Snow, being composed of ice grains of varying shapes, sizes, orientations, etc., has been treated as a particulate material. The mechanical properties of snow have been described in terms of microstructural parameters. A set of variables, which characterise the microstructure of snow at the granular level, has been chosen and quantified following the techniques of quantitative stereology for section plane. The data of quasi-static tests, e.g. constant strain-rate and creep tests, have been analysed to determine the Young's modulus and compactive viscosity and the same have been correlated with the microstructural parameters. Inspite of scatter, definite trends are discernible.

Considering the fact that deformation of snow is associated with translation and rotation of constituent grains in such a way as to attain the most stable configuration, the concept of fabric reconstruction, which is characterised by the concentration of normals (to the tangent plane at the point of grain contact) in the direction of the applied load, has been examined. The results demonstrated the occurrence of fabric reconstruction during the process of deformation. Finally, a dimensionless quantity, called the microstructural index (I), has been proposed to adequately represent the influence of microstructure.

INTRODUCTION

Snow is composed of ice grains of varying shapes and sizes, dispersed in a matrix of air and or water making snow to be categorised as a particulate material. Density has long been used to define the mechanical as well as physical properties of snow. However, the particulate nature of snow demands more rigorous treatment. Modern constitutive theories lay emphasis on the use of microstructural parameters. The problem thus centres around the selection and measurement of microstructural parameters and then identification of the dependence of the mechanical properties on the microstructural parameters.

Kry[1], Gubler[2], Hansen[3] and Quest[4] have carried out extensive work to identify significant internal state variables which represent the microstructure of snow under finite deformation. It has been recognised that the selected variables describe the microstructural features of the material besides representing average measure of the structural rearrangement. The variables are also capable of adequately describing the dominant deformation mechanism and account for various phenomena known to occur during compressive loading. On the other hand, except for the work of Kry[1] and Quest[4], there is a gap in knowledge relating influence of the microstructure on the mechanical properties. This paper aims to highlight these relationships. While the measurement of the variables followed the techniques described by Hansen[3] and Quest[4], the mechanical properties, i.e. Young's modulus (E) and compactive viscosity (η) have been

evaluated from quasi-static constant strain rate and creep tests under uniaxial compression. E and η are determined by analysing the creep data in terms of Burger's body. In spite of scatter, definite trends are discernible.

Snow undergoes large volumetric strains, which are largely irreversible. During plastic deformation, the granular structure of snow changes drastically. Intergranular pores close and grains as well as grain bonds fracture. These processes cause reorientation of the grains. The deformation of snow is thus considered to be associated with translation and rotation of constituent grains, such that they attain the most stable configuration. This implies that fabric reconstruction takes place. Drawing on the theories suggested by Oda[5-7] for sand, fabric reconstruction in snow has been examined and presented in this paper. A dimensionless parameter, which describes the material adequately at the granular level, has also been suggested.

2. THEORETICAL DEVELOPMENT

2.1 Structural Characteristics

The physical and mechanical properties of particulate materials are characterised by four groups of factors, viz. (a) the character of the basic structural units, (b) the geometrical arrangement of the structural units and the pore spaces, (c) the nature of the bonds between the structural units, and (d) the internal stresses. In case of snow, ice grains, cluster of ice grains and the chains of ice grains constitute the structural units. Given below is a brief overview of the factors mentioned above.

2.1.1 Character of Structural Units

It embraces the individual as well as the group characteristics of the structural units. The hardness, shape, size, roughness, grain-size distribution, etc. are the characteristics of significance and are usually termed as descriptive (or index) properties. Generally these are not considered as state-quantities as they can be studied on disturbed samples. However, in case of snow, variations in the characteristics of even these factors add to the complexity. Further, the difficulties associated with the measurements of these properties exclude the possibility of considering all of them except the size.

2.1.2 Geometrical Arrangement

Geometrical arrangement of the structural units of the solid phase of a particulate material is defined by the term 'fabric'. It is defined as the spatial arrangement of solid particles and associated voids. Oda[7] has defined the fabric of homogeneous granular material by two elements, viz., (i) orientation of individual particles called 'orientation fabric' and (ii) mutual relationship of the particles with each other called 'packing', as shown in Fig. 1.
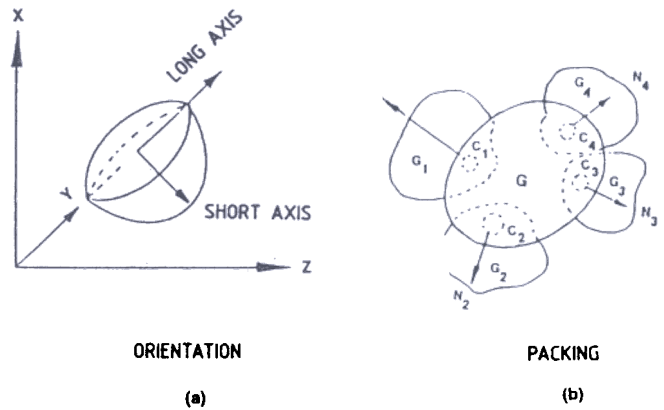

ORIENTATION

(a)

PACKING

(b)

Figure 1. Concept of fabric in granular material.

(a) Orientation fabric : It is the inclination of the true long axes of the particles to the reference direction as shown in Fig. 1(a). Due to the difficulty associated with the identification of the true long axis, it is customary to determine the inclination of apparent long axes of different grains to a reference direction in a vertical (V) or a horizontal (H) section plane. The distribution of the inclination of apparent long axes drawn as a histogram helps in the identification of the material characteristics.

(b) Packing : Figure 1(b) demonstrates the concept of packing. It is represented by two elements, viz., (i) the inclination of the normals, e.g. N_1, N_2, N_3, etc. to the tangent plane at the points of contact and (ii) the number of grain contacts, called the 'coordination number'. The first element in an assembly of many particles is expressed by a probability density function E (ψ,β) of the normals N_i. The second element is expressed by the mean and standard deviation of the coordination number.

(c) Probability density function, E (ψ,β) : The direction of a normal at the contact point of the two
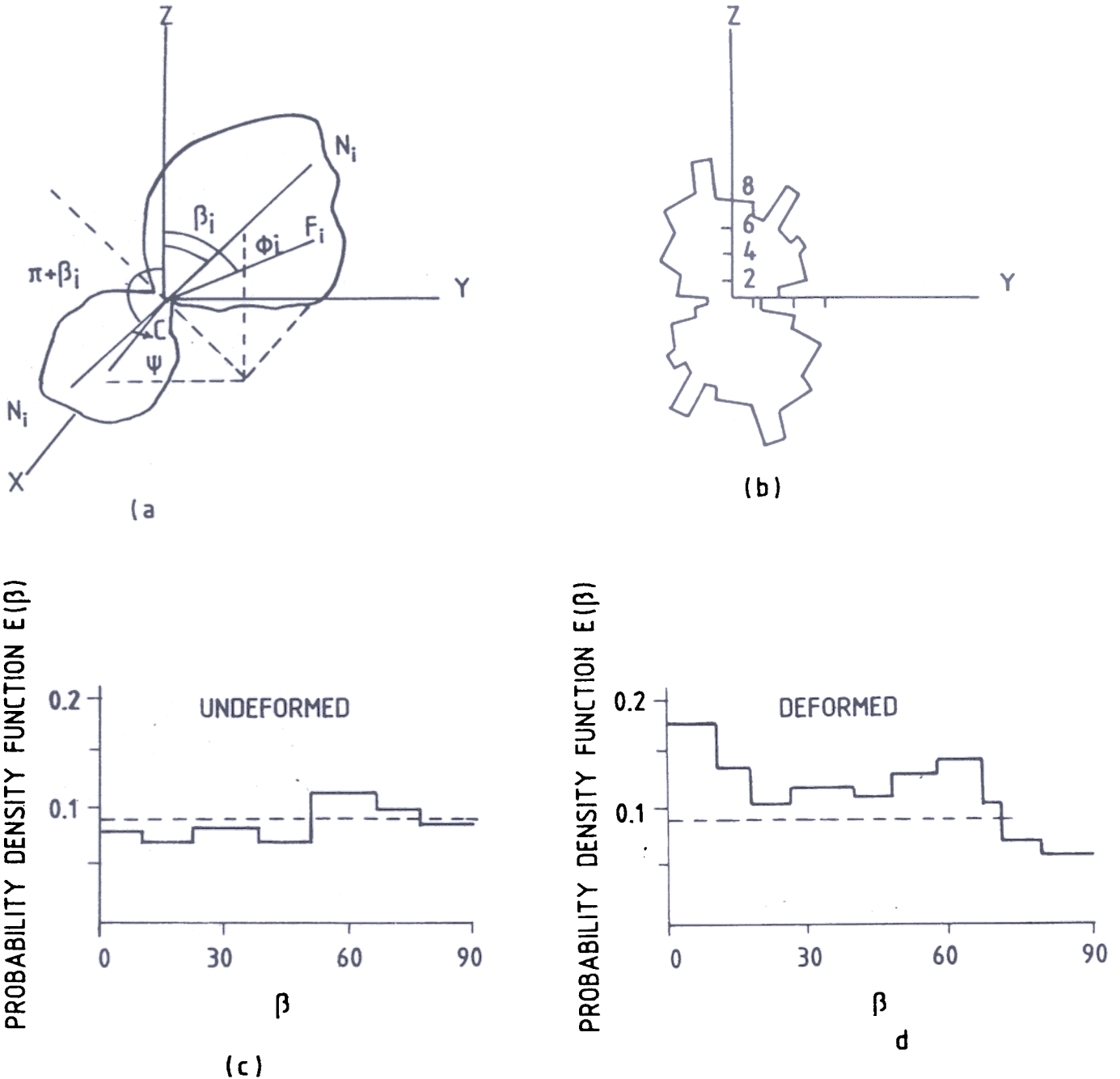
Figure 2. (a) Inclination angle of normals (N_i) at contact points, (b) Rose diagram showing distribution of N_i for *V/H* section, and (c) & (d) Probability density function $E(\beta)$ with respect to β for undeformed and deformed samples.

grains is defined by a set of angles denoted by ψ and β as shown in Fig. 2. However, the axial symmetry makes $E(\beta)$ to adequately represent $E(\psi,\beta)$. Following Oda[8], $E(\beta)$ can be calculated using the following expression:

$$E_1(\beta) = \frac{M_1}{4\pi M (\cos\theta_1 - \cos\theta_2)} \qquad (1)$$

where M_1 is the number of contacts between the grains in the solid angle θ_1 to θ_2 and M is the total number of contacts in the granular assembly. The other values of $E(\beta)$, i.e. $E_2(\beta)$, $E_3(\beta)$, etc. can be calculated in the same manner. However, under the conditions of isotropy, $E(\beta)$ has a constant value of $1/4\pi$.

95

(d) Mechanism of strain hardening : Oda[9], while investigating the mechanical properties of sand, observed the changes in the orientation fabric during deformation. He summarised that the non-spherical particles translate and rotate to take up the most stable position under the condition of applied stress. As a consequence of rearrangement, fabric reconstruction takes place. This is characterised by the concentration of the normals (N_i) in the direction of the axial stress (σ) as shown in Fig. 3. Oda, therefore, suggested that the contacts whose normals are parallel to the direction of applied stress must be more effective in supporting

Figure 3. Fabric reconstruction.

the axial stress. He concluded that the gradual concentration of N_i direction towards the load axis seems to be due to the construction of the columns in a granular assembly (Fig. 3). This suggests that the ability to support axial stress may gradually increase with the decrease in angle β. This results in apparent strain hardening of the material till the failure, after which the process recommences. This explains the characteristic saw-tooth pattern of load-displacement diagram.

(e) Coordination number : It represents the number of bonds or contacts each grain makes with the neighbouring grains. Various techniques have been suggested to determine the coordination number. All these methods make use of 2D-parameters measured from section plane along with an assumption of grain

shape. Dehoff and Rhines[10] have, however, shown that relatively small variation in assumed grain geometry with actual shape can lead to considerable error. Gubler's method[2] of determining coordination number requires a number of parameters including the shape factor. Hansen[3] introduced normalising constants in the determination of two-dimensional as well as three-dimensional probability distribution function of a grain. He identified that the probability (that if a grain with coordination number $N_3 = 1$ is cut by a section plane, its bond also lies in the section plane) is a function of N_{gv} (number of grains per unit volume) and hence it would be more appropriate to vary 'N_{gv}' and adjustable free index i instead of N_3 and i. This eliminates the use of shape factor.

2.1.3 Grain Bonds

Ice grains, the main constituent of snow, first interlock and bond, then transform into simpler forms over a period of time. Snow of this type gains strength. On the other hand, ice grains do not bond well under extremely low temperature conditions (below -20 °C). Dry granular materials exhibit the characteristics of friction bond under the state of non-zero stress. A similar behaviour is expected when the snow pack comprises depth hoar grains. Snow, under such a condition, lacks shear strength. However, under relatively favourable conditions when grain bonding takes place during destructive metamorphism, generally a brittle structure evolves due to the formation of brittle cohesive bonds. In such cases, even a small displacement of two particles relative to each other is enough to cause failure of bonds. In view of the fact that the dominant deformation mechanisms are pore collapse, bond fracture, intergranular glide, etc. and that the neck and bond growth also takes place due to sintering, grain bonding acquires immense significance in particulate materials, more so in snow.

The definition of grain bonds given by Kry[11] has been used in the current work. He assumed it to appear like a circular disc, when sectioned through it. He suggested three criteria: (i) there must be a minimum constriction of ice in the section plane, (ii) constriction must be present on both edges of ice grain and (iii) constrictions must point approximately towards each other as shown in Fig. 4. The definition of neck as extended by Hansen has been used. He idealised necks
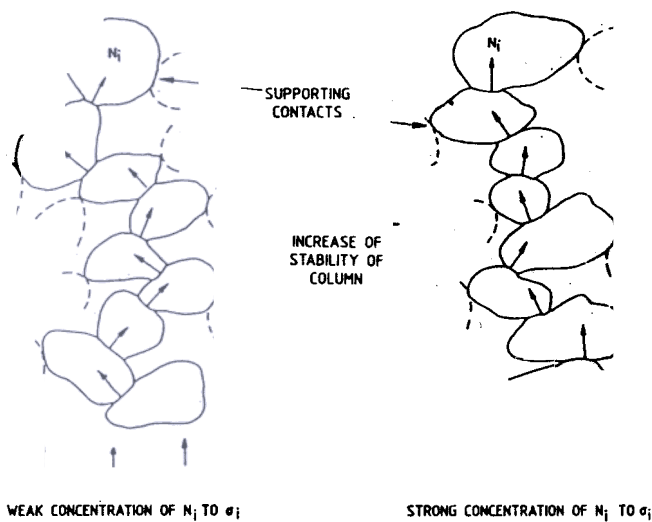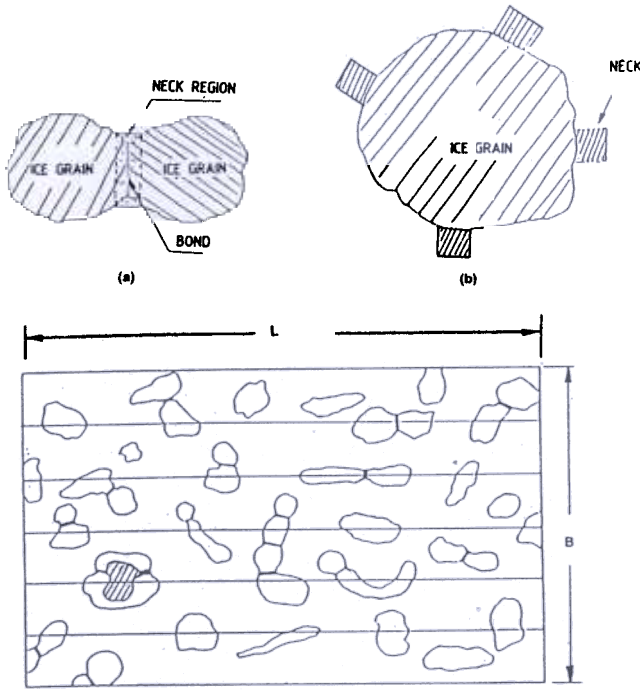
Figure 4. (a) Idealised picture of ice grain, bond & neck, (b) idealised grain with necks, and (c) sketch showing section plane.

as cylinders of ice, which connect two grains. However, the following limitations are recognised:

(a) It is easier to distinguish bond/neck in all those cases in which the individual grains are clearly discernible, however, when either the grains tend to merge into each other or bonds grow into the grain, distinction between the grains and bonds becomes difficult. This is significant in case of needles and highly metamorphosed materials.

(b) Nuclei, inclusions and air bubbles tend to make bond identification unsatisfactory, and

(c) Neck region delineation is very subjective.

2.2 Microstructural Parameters

Hansen identified significant internal state variables which represent the microstructure of snow under finite deformation. Snow has been assumed to be a homogeneous, isotropic three-phase mixture of air, grain and neck/bond. The techniques of quantitative stereology have been applied to determine 3-D parameters using 2-D measurements made from section plane. It has also been identified that either of the three methods of counting, viz., point, line and area, can be employed to determine 3-D microstructural parameters,

however point counting technique is considered to be superior.

2.2.1 Two-Dimensional Measurements

The following measurements of 2-D parameters, as shown in Fig. 4, have been made from section planes:

(a) N : Total number of grains in the test area
(b) n : Total number of bonds in the test area
(c) D_{2i} : Bond diameter of i-th bond
(d) L_T : Total length of all test lines
(e) A : Total test area
(f) l : Total length of grain intercepts
(g) A_b : Area of bonds, and
(h) A_g : Area of grains.

Using the foregoing, the following 2-D parameters have been computed:

(a) $N_{gL} = N/L_T$: Number of grains per unit length of test line
(b) $N_{gA} = N/A$: Number of grains per unit test area
(c) $N_{bA} = n/A$: Number of bonds per unit test area
(d) $l_{LT} = l/LT$: Line fraction
(e) $A_{gA} = A_g/A$: Area of grains per unit test area
(f) $A_{bA} = A_b/A$: Area of bonds per unit test area,
(g) $a = \dfrac{\rho_{ice}}{\rho}$: Density ratio ρ_{ice} and ρ are densities of ice and snow, respectively

$$= \frac{1}{A_{gA} + A_{bA}} \quad \text{and}$$

(h) $H = \dfrac{1}{n}\Sigma\dfrac{1}{D_{2i}}$: Harmonic mean

2.2.2 Three-Dimensional Parameters

The 3-D parameters have been computed as under. This uses a modified definition of free grain-surface area per unit volume.

(a) Mean bond radius (R_3):

$$R = \frac{\pi}{\_\_\_\_}$$

(b) Mean pore length (λ

$$\lambda = \frac{a-1}{aN_{ol}}$$

(c) Mean intercept length (L

$$L = \frac{l_{LT} + A_{bA}}{N_{gL}}$$

(d) Mean number of bonds per unit volume (N_{bv})

$$N_{bv} = \frac{8HN_{bA}}{\pi^2}$$

(e) Mean neck length (h)

$$h = \frac{A_{bA}}{\pi N_{bv} R_3^2}$$

(f) Mean free grain-surface area per unit volume (S_v). Underwood[12] showed that the surface area of a detached grain is given by $4N_{gL}$. Cross-sectional area of each bond of radius R_3 is πR_3^2, accounting for the number of bonds per grain (N_3), and the total number of grains per unit volume (N_{gv}), ($\pi R_3^2 N_3 N_{gv}$) gives the area covered by all bonds. Thus the free grain-surface area is given by:

$$S_v = 4N_{gL} - \pi R_3^2 N_3 N_{gv} \tag{2}$$

While computing the foregoing parameters, considerations of grain shape are not required. The determination of N_{gv} and N_3 needs to take into account the grain shape factor. Realising that any attempt to characterise alpine snow by a grain shape factor is unlikely to be successful due to wide range of shapes, the approach suggested by Hansen and slightly modified by Quest, which does not require the shape factor, has been used. The software written by Hansen and modified by Quest has been used to evaluate the values of N_{gv} and N_3.

2.3 Mechanical Properties

Young's modulus (E) and compactive viscosity (η) have been selected to represent the material behaviour. The mechanical properties have been determined by assuming the material response to be linear viscoelastic.

Constant strain rate and creep test results have been used to determine E and η. In the constant strain rate tests, samples are strained at rates varying between $10^{-5}\ s^{-1}$ and $10^{-4}\ s^{-1}$ for 5 s to ensure that the total strain remains less than 0.2 per cent. The average slope of the plots between stress (σ) and strain (e) is taken to represent the Young's modulus.

In the next step, the data of creep tests, performed on the same sample on which constant strain rate tests are performed are analysed in terms of Burger's-body solution as given by the following expression :

$$e(t) = \sigma_0 \left\{ \frac{1}{E_1} + \frac{t}{\eta_1} + \frac{1}{E_2} \left(1-e \left(-\frac{E_2}{\eta_2} t \right) \right) \right\} \tag{3}$$

The value of E determined from constant strain rate tests is taken as the initial guess to obtain the value of all the constants of Eqn (3). Although this helps in minimising the problem of solution stability, yet the uniqueness of the solution continues to be a problem.

2.4 Microstructural Index

As discussed in the preceding paragraphs, the properties of snow depend on the character, the geometrical arrangement of the structural units and pore spaces, the nature of bonds between the structural units, etc. Thus an attempt to characterise the microstructure should include most of these parameters besides representing the dominant deformation mechanisms. L_3 has been assumed to represent the grain character, N_{bv} has been taken to describe the bond and S_v is considered to reflect the combined effects of grain geometry and bond character. Thus a dimensionless quantity $S_v/N_{bv} L_3^2$ has been identified to represent the microstructure. This has been termed as microstructural index (I).

3. EXPERIMENTATION

3.1 Apparatus

A servo-control microprocessor-based, 10 kN Universal Testing Machine, made by Dartec Company, UK, has been used for the strain rate and creep tests measurements. A base sledge microtome has been used to prepare thick sections. An optical and a stereo-microscope each fitted with photographic facilities have been used to obtain micro-photographs for the determination of the microstructural parameters.

3.2 Sample Preparation

The snow collected from the field stations is sieved and transferred to a pre-lubricated sampler. The samples are allowed to sinter at -20 °C for periods varying between 6-20 days. The samples are first pre-compressed to an estimated density before allowing them to sinter. Conditioned samples are brought to desired density and are allowed to relax for a period of at least 10 times the duration for which they have been strained.

3.3 Test Procedure

Standardisation of the test procedure is given due attention. Constant strain-rate and creep tests are performed in confined compression. Samples of initial

density between 270 and 290 kg/m^3 are densified to 300 kg/m^3 at a constant strain-rate of 10 × 10^{-5} s^{-1} and then relaxed for 600 s. Constant strain-rate of 6 × 10^{-5}, 8 × 10^{-5} and 40 × 10^{-5} s^{-1} are applied for 5 s each. Samples are relaxed for 300-600 s before the application of next strain-rate. The samples are then subjected to creep test. Stresses of 0.015, 0.030, and 0.09 MPa are applied. Specimen are removed at different stages to examine the microstructure at sample densities of 320 and 360 kg/m^3 in addition to the ones at the beginning and the end of the test.

3.4 Examination of Microstructure

3.4.1 Preparation of Specimen

A 1.5 cm high specimen is cut off from the sample before it is subjected to compression tests. A square piece of approx 2 × 2 sq cm is cut off from the specimen and transferred to a steel tray of 4.5 × 4.5 ×0.9 cm size. The tray is filled with a pore filler. Laboratory grade di-methyl-phthalate is used. It is mixed with a water-insoluble dye for enhancing the contrast between ice grains and the pore space. Pore filler is generally maintained at -7 °C before pouring into the tray. Approximately 8 to 10 min are allowed for the pore filler to rise up the specimen by capillary action. In the absence of dry ice, the specimen are frozen in a cold chamber maintained at -20 °C. Solidification of the pore filler requires approx 24 h.

The tray is then clamped on base-sledge microtome and the specimen shaved. At first, a cut as large as 40 μm is given. The specimen surface is polished by gradually reducing the cut to about 2 μm. Considerable pitting is observed on many occasions. Microtoming is continued till pitting comes down to a minimum. Once an almost shining surface is achieved, the surface of the thick section is slowly polished with lense-cleaning tissue and left undisturbed for about 3 to 5 min. Polishing is never performed without the gloves as heat from the fingers tends to melt the grains. Vapour pressure gradient between the grain boundaries and the grain surface leads to etching of observable boundaries around ice-pore filler interface.

Contrast enhancement is achieved by applying water insoluble fingerprint black with a cotton swab and staining the ice grains with a water soluble dye. The specimen is now considered to be ready for photography. Gradual microtoming and patient

application of contrast-enhancing chemicals paid rich dividends in the preparation of thick section.

3.5 Microphotography

Microphotographs are taken using 320 ASA high speed cut films. An exposure of 8 s is given. Photographs are printed under a controlled temperature of 20 °C with a time of development of 3 min. Inadequate or non-uniform illumination renders the photographs unusable. Lamps are therefore so adjusted that an almost uniform illumination is achieved. Photographs are taken with 10X magnification and enlarged.

4. RESULTS AND DISCUSSION

4.1 Microstructural Parameters

A limited number of two-dimensional parameters are measured due to the non-availability of image analysing facilities. The micrographs are divided into two parts with approx 30 per cent overlap. Each part is analysed for microstructural parameters independently and the results are compared with each other. In view of the subjectivity associated with the marking of the necks, variations in results are unavoidable. Repeated analyses have been continued till the difference in the two parts came down to below 10 per cent. The following parameters were measured: (a) area of microphotographs, (b) number of grains, (c) total length of test lines, (d) number of grains intersected by test line, (e) total length of intercepts, (f) frequency distribution of bond diameters, (g) area of bonds, and (h) frequency distribution of the number of bonds.

Measurement of microstructural parameters has been made to investigate: (a) the fabric re-construction, (b) the influence of microstructural parameters on the mechanical properties, and (c) the dependence of power law exponent (γ) on the microstructure.

4.2 Fabric Re-construction

A number of experiments have been conducted on samples of initial density up to 360 kg/m^3. The samples are densified in various stages, vertical section planes are made and microphotographs taken. Inclination of the normals at the point of contact are measured with respect to the direction of the applied stress. The values of E (β) are calculated for a dispersion of 15° in the value of β. The plots between $E(\beta)$ and β are drawn. Simultaneously, rose diagrams representing the distribution of N_i have also been made.
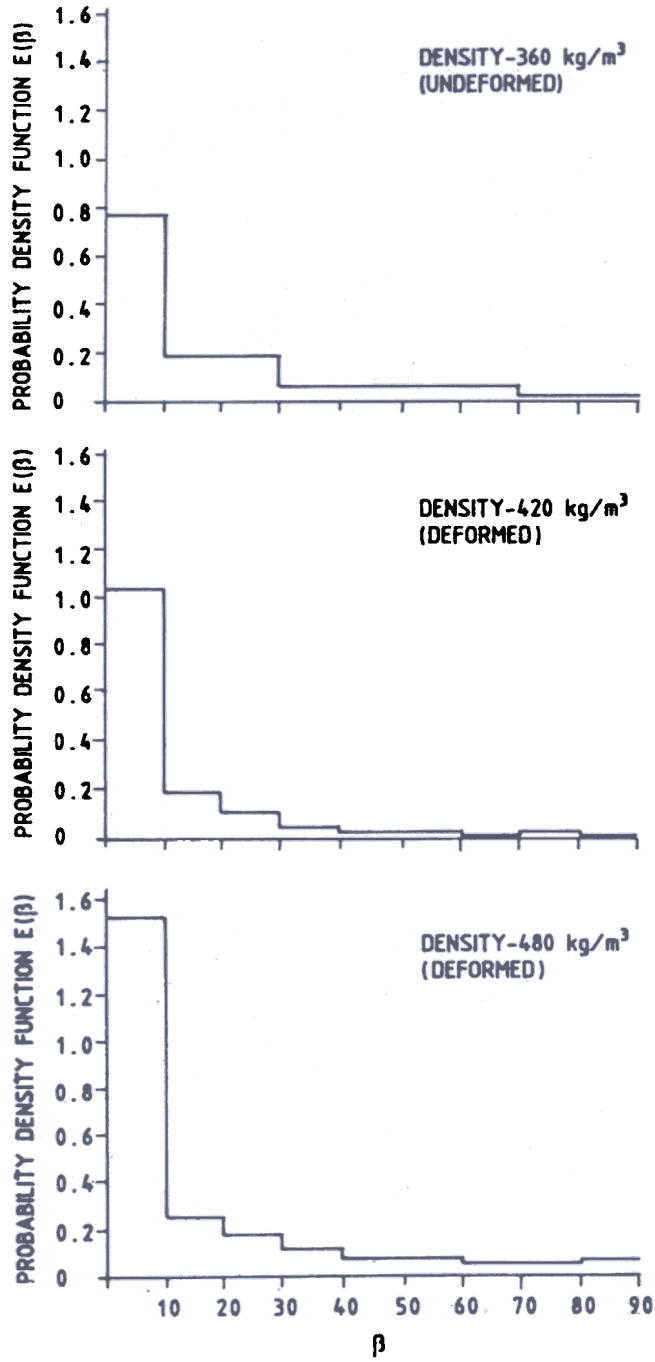
Figure 5. N_i distribution, probability density function $E(\beta)$ vs β.

Figure 5 presents a histogram showing the variation of $E(\beta)$ with β as the density of the sample changes from 360 kg/m^3 in undeformed state to 480 kg/m^3 as a result of progressive deformation. The increase in $E(\beta)$ in the range of 0 to 30 degree with the progressive deformation process clearly demonstrates the process of fabric re-construction during deformation. Figure 6 shows the progressive change in the frequency
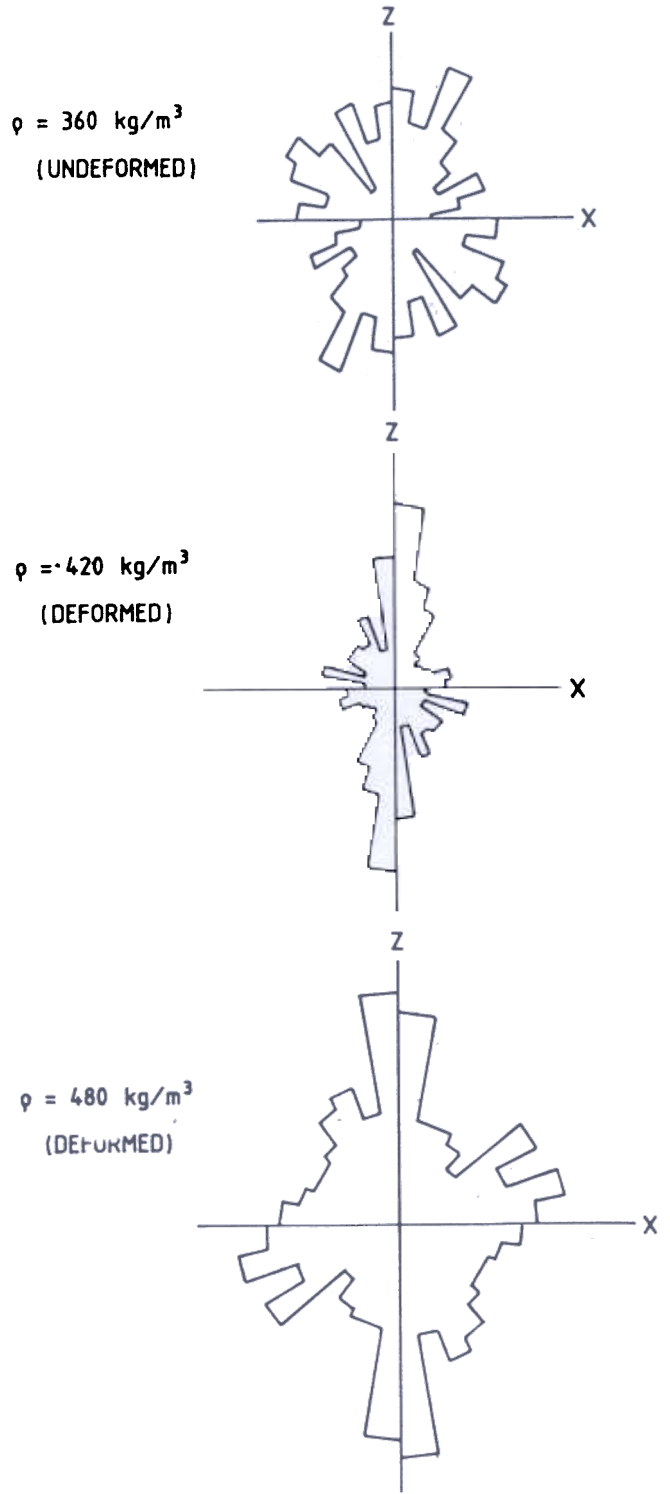
Figure 6. Progressive change in frequency distribution of N_i during uniaxial confined compression.

distribution of N_i, as a result of uniaxial confined compression. This also shows an explicit rotation of the normals towards the load axis, which demonstrates rotation of the grains to achieve most stable orientation

with a view to adjusting to the changed state of stress. It can thus be concluded that the fabric re-construction is an important phenomenon in the deformation mechanism of snow.

4.3 Microstructure *vs* Mechanical Properties

Many workers have identified the significance of microstructure. Kry was, however, the first to apply the techniques of stereology to quantify the microstructural parameters and suggest their influence on the Young's modulus and viscosity. In the present work, authors have attempted to find dependence of the mechanical properties on the microstructural parameters. The results of analysis of the dependence of Young's modulus and compactive viscosity on microstructural parameters are presented in Figs 7 to 12.

4.3.1 Young's Modulus

The degree of bonding between grains and pore length (or the mean free distance between grains) are considered to control the mechanical properties. Connected with these are the number of grains and bonds per unit volume as well as the free grain surface area per unit volume. The larger the number of bonds and/or bigger the radius, the higher the resistance the material offers to the deformation and higher will thus be the Young's modulus.

(a) E vs (λ) and (λ/L₃) : Figures 7(a) and 7(b) show the dependence of Young's modulus on mean free distance between the grains (λ) and the grain mobility (λ/L_3), respectively. It can be easily visualised that the ability to resist deformation with the increase in (λ) and grain-mobility (λ/L_3) decreases. The material tends to behave like a liquid, which keeps deforming under the smallest load. Inspite of the scatter, the two plots show very clearly a linear relationship of (λ) and (λ/L_3) with E.

(b) E vs N₃ & R₃ : Grain bonds are the locations of largest constriction relative to grain itself. These are, therefore, zones of highest stress concentration. The grain bond radius R_3 and the coordination number N_3, thus play a key role in determining the load bearing ability of the sample. An increase in the value of N_3 and R_3 should show an increase in the value of the modulus. Figure 8(a) shows that the modulus value increases parabolically with the increase in R_3. This appears logical as the modulus is expected to be directly
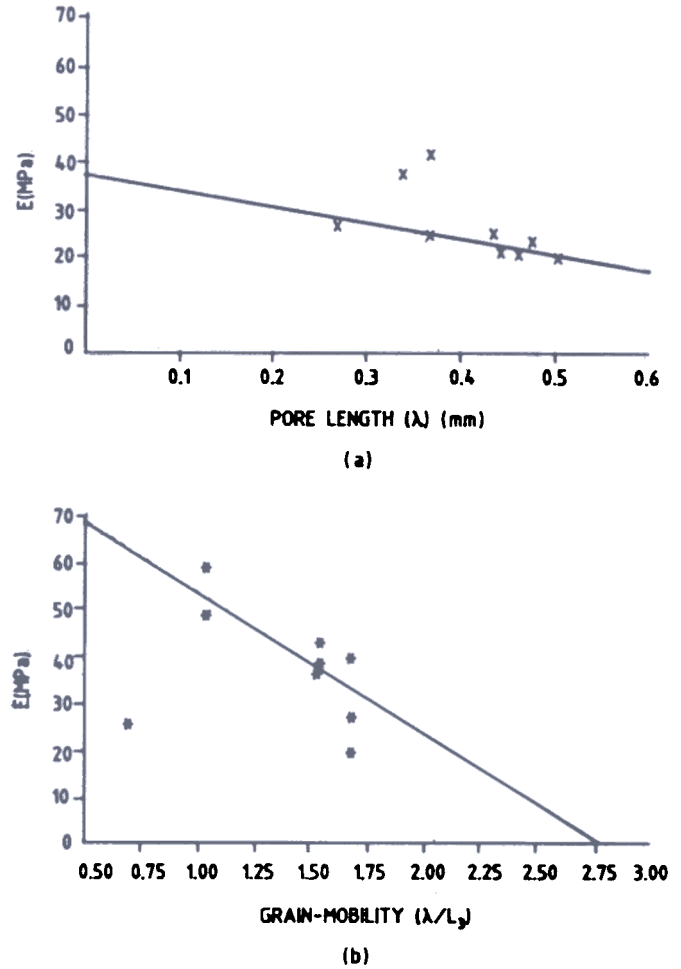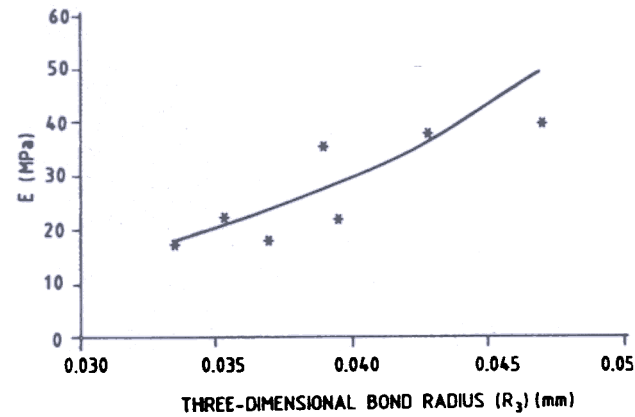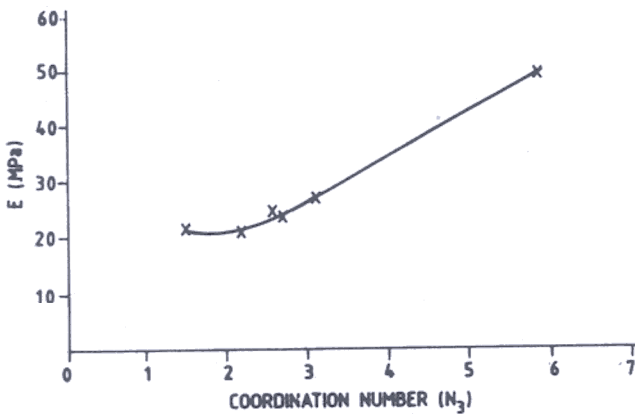

Figure 7. Dependence of Young's modulus (E) on (a) pore length and (b) grain mobility (λ/L₃).

dependent on contact area of the grains (πR_3^2). Figure 8(b) shows that the value of E increases first slowly and then rapidly with the increase of the coordination number N_1.

(c) E vs Sᵥ : The mean free grain-surface area per unit volume (S_v) is directly related to the packing. Higher the coordination number, higher will be number of grains per unit volume and smaller will be the free grain-surface area. As this condition increases the ability to resist higher stress, an increase in free grain-surface area would lead to the loss of modulus. Figure 9(a) first shows rapid decrease of E with the increase in mean free grain-surface area, which may be the result of either higher porosity or breaking of the bonds. It also shows a limiting value of the Young's modulus which implies that the material is expected to have a minimum modulus of elasticity.
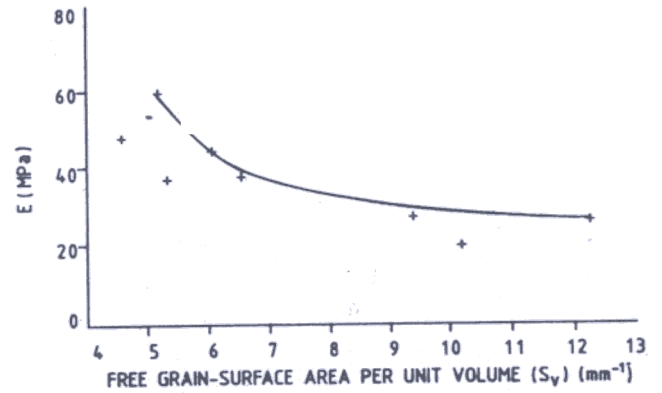
Figure 8. Dependence of Young's modulus (E) on (a) three-dimensional bond radius (R_3), and (b) coordination number (N_3).

Figure 9. Dependence of Young's modulus (E) on (a) free grain-surface area per unit volume (S_v), and (b) microstructural index (I).
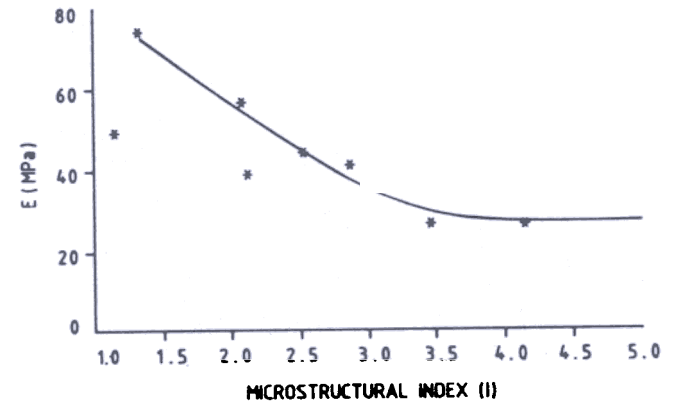
(d) E vs I : Figure 9(b) presents a plot between E and the microstructural index I. It shows a decreasing trend in the value of E with the increase in the value of I. An increase in the value of N_{bv} will cause decrease in the value of S_v, L_3 may or may not be affected. However, the change in L_3 will always be relatively smaller. Thus the combined affect of the three parameters will always be more drastic than that of any one of them individually. It is because of this phenomenon that the plot first shows a rapid decrease in the value of E with the increase in value of I as compared to S_v. It also gives a limiting value of E.

4.3.2 Compactive Viscosity

The viscous element (dashpot) of Maxwell's unit in the Burger's body has been assumed to represent the viscosity of the material. An attempt has been made to

establish a qualitative relationship of η with the microstructural parameters of the material.

(a) η vs λ & λ/L_3 : Although, the causes of viscous flow in snow are not well understood, yet higher pore-space imparts greater grain mobility and hence lesser resistance to flow. Thus higher the mean free distance between the grains (λ), higher will be the likelihood of grain-mobility (λ/L_3) and hence lesser will be the material viscosity. Figures 10(a) and 10(b) show the same trends.

(b) η vs R_3 : Grain bonds are the regions of maximum stress concentration. On the application of stress, grain bonds first deform and then give way. Frequency distribution of the grain bond diameter shows that smaller-diameter bonds predominate over larger-diameter bonds. A decrease in bond diameter affects an increase in intergranular glide. This implies that a reduction in the bond diameter decreases
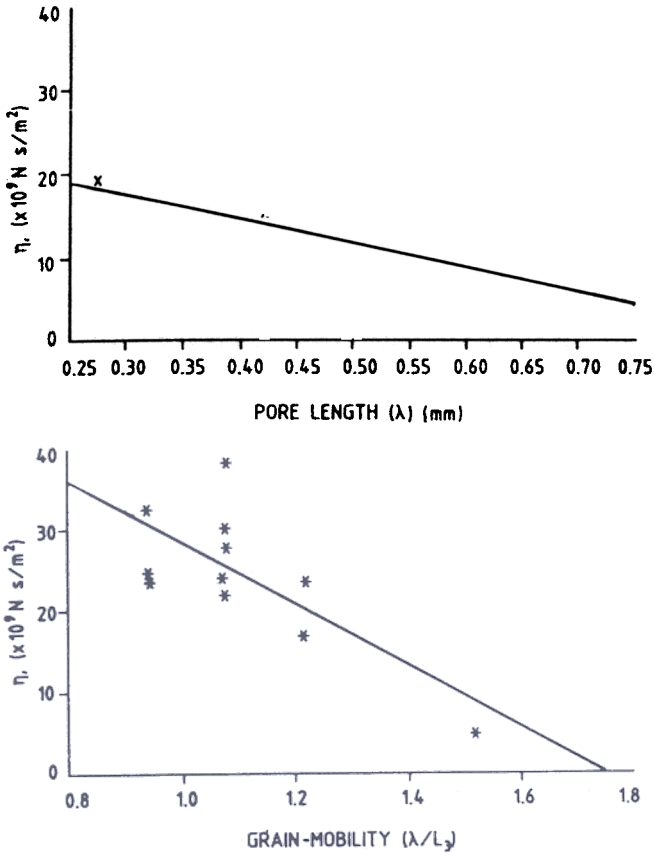
Figure 10. Dependence of viscosity (η) on (a) pore length (λ) and (b) grain-mobility (λ/L_3).

resistance to flow and hence reduces the viscosity. Experimental results plotted in Fig. 11(a) show an increase in viscosity (η) with the increase in average bond-radius (R_3).

(c) η *vs* N_{bv} : As argued in the case of modulus, the number of bonds per unit volume influences the
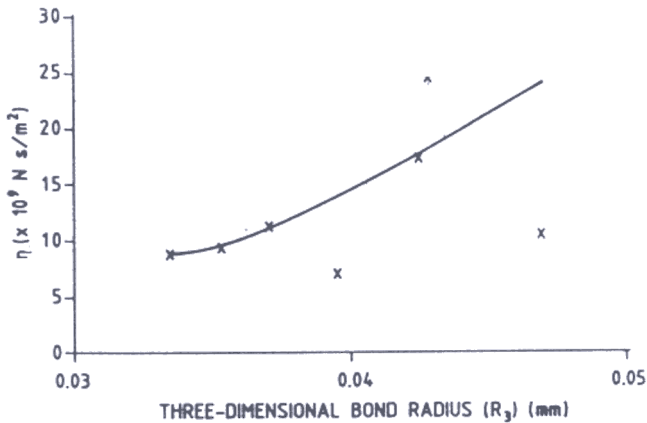

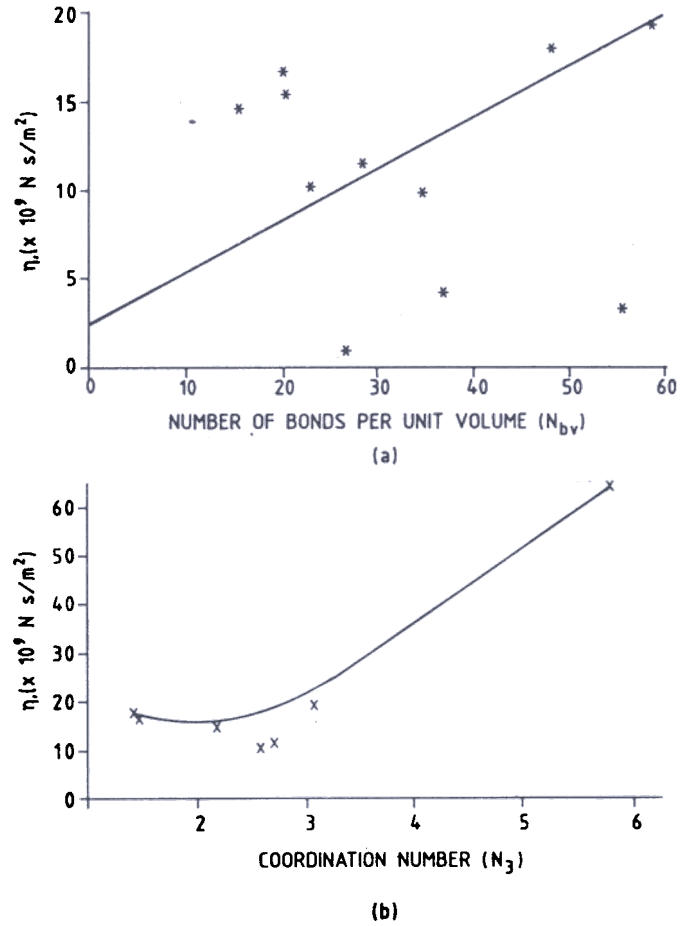Figure 11. Dependence of viscosity (η) on three-dimensional bond radius (R_3)

Figure 12. Dependence of (η) on (a) number of bonds per unit volume (N_{bv}) and (b) coordination number (N_3).

viscosity too. The higher the number of bonds, the lesser will be the grain mobility and lesser will, therefore, be the intergranular glide. Thus an increase in N_{bv} will cause an increase in viscosity. Figure 12(a) shows an increasing trend.

(d) η *vs* N_3 : As the densification proceeds, more and more grains get packed in a unit volume and the coordination number increases. An increase in the coordination number reduces the grain mobility and hence the intergranular glide. Thus an increase in N_3 will resist the flow and hence cause an increase in viscosity. Figure 12(b) presents the same trend. Almost constant value of viscosity for low coordination number must be associated with a relatively higher grain-mobility.

(e) η *vs* S_v : A decrease in free grain-surface area is related to the increase in the coordination number and the bond radius. Thus a plot between S_v and η is
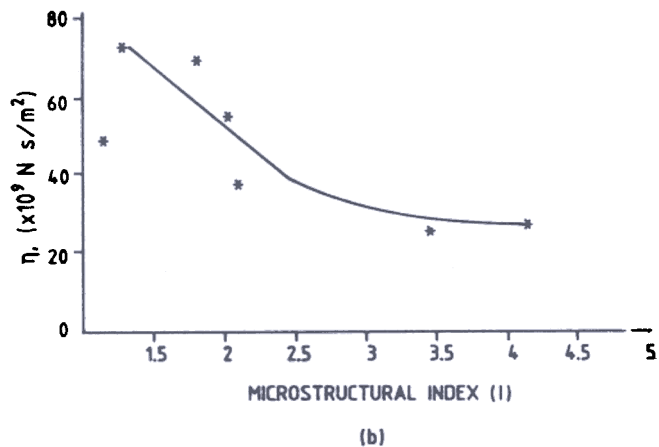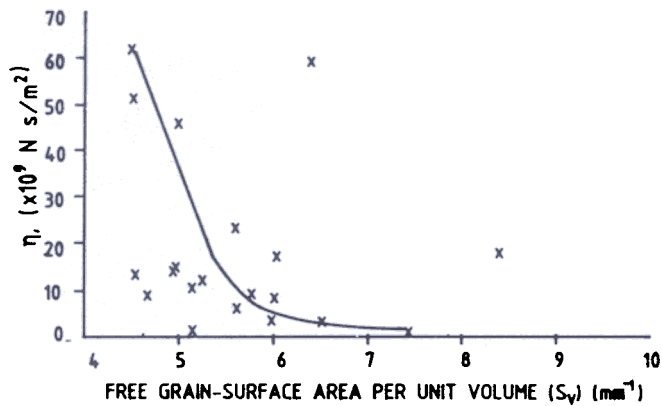
103

Figure 13. Dependence of (η) on (a) free grain-surface area per unit volume (S_v) and (b) microstructural index (I).

of fabric reconstruction recommences. This explains the reasons for saw tooth pattern of response characteristics of snow on the granular level. Inspite of considerable scatter, the ˙results show explicit influence of microstructure on Young's modulus (E) and compactive viscosity (η) consistent with the physical processes responsible for deformation. The results also indicate that a single parameter, called microstructural index I, can be well correlated with the mechanical properties of the material; they however, highlight the necessity of conducting further experiments to suggest quantitative relationships.

ACKNOWLEDGEMENT

expected to show opposite trends when compared to that of the trends for N_3 and R_3. Figure 13(a) shows first a relatively sharper reduction in viscosity with the increase in S_v, which then levels off. Asymptotic pattern indicates that the material retains a definite viscosity, as in the case with modulus.

(f) η vs I :   The dependence of the dimensionless index (I) on the viscosity shows almost a similar behaviour as found for the modulus except that decrease is relatively sharper (Fig. 13(b)).

5. CONCLUSION

In conclusion, it is noted that snow demonstrates fabric reconstruction during the process of deformation. This results in increased stress bearing ability. However, the structure gives way at a certain stage and the process

REFERENCES

1. Kry, P.R. The relationship between the viscoelastic and structural properties of fine grained snow. *J. Glaciol.*, **14**(72), 1975.

2. Gubler, H. Determination of the mean number of bonds per snow grain and the dependence of the tensile strength of snow on stereological parameters. *J. Glaciol.*, **20**(83), 1978.

3. Hansen, A.C. A constitutive theory for high rate multi-axial deformation of snow, MSU, Montana, USA, 1985, PhD Thesis.

4. Quest, E. Determining the change in snow microstructure during large deformation process by the method of quantitative stereology, MSU, Montana, USA, 1989, MS Thesis.

5. Oda, M. Initial fabric and their relations to mechanical properties of granular material. *Soil Fdn.*, 1972, **12**(1), 17-36.

6. Oda, M. The mechanism of fabric changes during compressional deformation of sand. *Soil Fdn.*, 1972, **12**(4), 45-63.

7. Oda, M. Coordination number and its relation to shear strength of granular material. *Soil Fdn.*, 1977, **17**(2), 29-42.

8. Oda, M. Fabric tensor for discontinuous geological materials. *Soil Fdn.*, 1982, **22**(4).

9. Oda, M. Significance of fabric in granular mechanics. Proceedings of US-Japan seminar on the mechanics of granular material, Tokyo, Japan, 1978, 7-26.

10. DeHoff, R.T. & Rhines, F.N. Determination of number of particles per unit volume from measurement made on random plane sections: the general cylinder and the ellipsoid. *Trans. Metallurg. Soc. AMIE*, 1961, **221**, 975-82.

1 Kry, P.R. Quantitative stereological analysis of grain bonds in snow. *J. Glaciol*, 1975 **14**(72).

12 Underwood, E.E. Quantitative stereology. Addison-Wesley, Reading, Massachusetts, USA, 1970.